

Megafoods in Europe can be anticipated from observations in hydrologically similar catchments

Original

Megafoods in Europe can be anticipated from observations in hydrologically similar catchments / Bertola, M.; Blöschl, G.; Bohac, M.; Borga, M.; Castellarin, A.; Chirico, G. B.; Claps, P.; Dallan, E.; Danilovich, I.; Ganora, D.; Gorbachova, L.; Ledvinka, O.; Mavrova-Guirguinova, M.; Montanari, A.; Ovcharuk, V.; Viglione, A.; Volpi, E.; Arheimer, B.; Aronica, G. T.; Bonacci, O.; Canjevac, I.; Csik, A.; Frolova, N.; Gnanndt, B.; Gribovszki, Z.; Gul, A.; Gunther, K.; Guse, B.; Hannaford, J.; Harrigan, S.; Kireeva, M.; Kohnova, S.; Komma, J.; Kriauciuniene, J.; Kronvang, B.; Lawrence, D.; Ludtke, S.; Mediero, L.; Merz, B.; Molnar, P.; Murphy, C.; Oskorus, D.; Osuch, M.; Parajka, J.; Pfister, L.; Radevski, I.; Sauquet, E.; Schroter, K.; Sral, M.; Szolgay, J.; Turner, S.; Valent, P.; Veijalainen, N.; Ward, P. J.; Willems, P.; Zivkovic, N.. - In: NATURE GEOSCIENCE. - ISSN 1752-0908. - 16:11(2023), pp. 982-988. [[10.1038/s41561-023-01300-5](https://doi.org/10.1038/s41561-023-01300-5)]
Availability: This version is available at: <https://doi.org/10.1583/2984144> since: 2023-11-28T07:52:52Z

Publisher:

Springer Nature

Published

DOI:10.1038/s41561-023-01300-5

Terms of use:

This article is made available under terms and conditions as specified in the corresponding bibliographic description in the repository

Publisher copyright

(Article begins on next page)

Submitted to Nature Geoscience

Megafloods in Europe can be anticipated from observations in hydrologically similar catchments

Author list

Miriam Bertola^{1*}, Günter Blöschl¹, Milon Bohac², Marco Borga³, Attilio Castellarin⁴, Giovanni B. Chirico⁵, Pierluigi Claps⁶, Eleonora Dallan³, Irina Danilovich⁷, Daniele Ganora⁶, Liudmyla Gorbachova⁸, Ondrej Ledvinka^{2,9}, Maria Mavrova-Guirguinova¹⁰, Alberto Montanari⁴, Valeriya Ovcharuk¹¹, Alberto Viglione⁶, Elena Volpi¹², Berit Arheimer¹³, Giuseppe Tito Aronica¹⁴, Ognjen Bonacci¹⁵, Ivan Čanjevac¹⁶, Andras Csik¹⁷, Natalia Frolova¹⁸, Boglarka Gmandt¹⁷, Zoltan Gribovszki¹⁹, Ali Gül²⁰, Knut Günther²¹, Björn Guse^{21,22}, Jamie Hannaford^{23,24}, Shaun Harrigan²⁵, Maria Kireeva¹⁸, Silvia Kohnová²⁶, Jürgen Komma¹, Jurate Kriauciuniene²⁷, Brian Kronvang²⁸, Deborah Lawrence²⁹, Stefan Lüdtke²¹, Luis Mediero³⁰, Bruno Merz^{21,31}, Peter Molnar³², Conor Murphy²⁴, Dijana Oskoruš^{33,34}, Marzena Osuch³⁵, Juraj Parajka¹, Laurent Pfister³⁶, Ivan Radevski³⁷, Eric Sauquet³⁸, Kai Schröter³⁹, Mojca Šraj⁴⁰, Jan Szolgay²⁶, Stephen Turner²³, Peter Valent¹, Noora Veijalainen⁴¹, Philip J. Ward^{42,43}, Patrick Willems⁴⁴, Nenad Zivkovic⁴⁵.

Affiliations

¹Institute of Hydraulic Engineering and Water Resources Management, Technische Universität Wien, Vienna, Austria.

²Czech Hydrometeorological Institute, Prague, Czechia.

³Department of Land, Environment, Agriculture and Forestry, University of Padova, Padua, Italy

⁴Department of Civil, Chemical, Environmental and Materials Engineering (DICAM), Università di Bologna, Bologna, Italy.

⁵Department of Agricultural Sciences, University of Naples Federico II, Naples, Italy.

⁶Department of Environment, Land and Infrastructure Engineering (DIATI), Politecnico di Torino, Turin, Italy.

⁷Climate Research Laboratory, Institute for Nature Management, The National Academy of Science of Belarus, Minsk, Belarus.

⁸Department of Hydrological Research, Ukrainian Hydrometeorological Institute, Kyiv, Ukraine.

⁹Department of Physical Geography and Geoecology, Faculty of Science, Charles University, Prague, Czechia.

¹⁰University of Architecture, Civil Engineering and Geodesy, Sofia, Bulgaria.

¹¹Hydrometeorological Institute, Odessa State Environmental University, Odessa, Ukraine.

¹²Department of Engineering, University Roma Tre, Rome, Italy.

¹³Swedish Meteorological and Hydrological Institute, Norrköping, Sweden.

¹⁴Department of Engineering, University of Messina, Messina, Italy.

¹⁵Faculty of Civil Engineering, Architecture and Geodesy, Split University, Split, Croatia.

¹⁶Department of Geography, Faculty of Science, University of Zagreb, Zagreb, Croatia.

¹⁷General Directorate of Water Management, Budapest, Hungary.

¹⁸Department of Land Hydrology, Lomonosov Moscow State University, Moscow, Russia.

- ¹⁹University of Sopron, Faculty of Forestry, Institute of Geomatics and Civil Engineering, Sopron, Hungary.
- ²⁰Department of Civil Engineering, Faculty of Engineering, Dokuz Eylul University, Izmir, Turkey.
- ²¹Helmholtz Centre Potsdam, GFZ German Research Centre for Geosciences, Section Hydrology, Potsdam, Germany.
- ²²Department of Hydrology and Water Resources Management, Institute for Natural Resource Conservation, Kiel University, Kiel, Germany
- ²³Centre for Ecology and Hydrology, Wallingford, UK.
- ²⁴Irish Climate Analysis and Research Units (ICARUS), Department of Geography, Maynooth University, Maynooth, Ireland.
- ²⁵Forecast Department, European Centre for Medium-Range Weather Forecasts (ECMWF), Reading, UK.
- ²⁶Department of Land and Water Resources Management, Faculty of Civil Engineering, Slovak University of Technology in Bratislava, Bratislava, Slovakia.
- ²⁷Lithuanian Energy Institute, Kaunas, Lithuania
- ²⁸Department of Ecoscience, Danish Centre for Environment and Energy, Aarhus University, Aarhus, Denmark.
- ²⁹Norwegian Water Resources and Energy Directorate, Oslo, Norway.
- ³⁰Department of Civil Engineering: Hydraulic, Energy and Environment, Universidad Politécnica de Madrid, Madrid, Spain.
- ³¹Institute of Environmental Sciences and Geography, University Potsdam, Potsdam, Germany
- ³²Institute of Environmental Engineering, ETH Zurich, Zurich, Switzerland.
- ³³Department of Hydrotechnics, Faculty of Geotechnical Engineering, University of Zagreb, Varaždin, Croatia.
- ³⁴Croatian Meteorological and Hydrological Service, Zagreb, Croatia.
- ³⁵Department of Hydrology and Hydrodynamics, Institute of Geophysics Polish Academy of Sciences, Warsaw, Poland.
- ³⁶Luxembourg Institute of Science and Technology (LIST), Esch-sur-Alzette, Luxembourg.
- ³⁷Institute of Geography, Faculty of Natural Sciences and Mathematics, Ss. Cyril and Methodius University, Skopje, North Macedonia.
- ³⁸Irstea, UR RiverLy, Lyon-Villeurbanne, France.
- ³⁹Leichtweiss Institute for Hydraulic Engineering and Water Resources, Technische Universität Braunschweig, Braunschweig, Germany.
- ⁴⁰Faculty of Civil and Geodetic Engineering, University of Ljubljana, Ljubljana, Slovenia.
- ⁴¹Finnish Environment Institute, Helsinki, Finland.
- ⁴²Institute for Environmental Studies (IVM), Vrije Universiteit Amsterdam, The Netherlands.
- ⁴³Deltares, Delft, The Netherlands.
- ⁴⁴Department of Civil Engineering, KU Leuven, Leuven, Belgium.
- ⁴⁵Faculty of Geography, University of Belgrade, Belgrade, Serbia.
- * Corresponding author. E-mail: bertola@hydro.tuwien.ac.at

Abstract

Mega-floods that far exceed previously observed records often take citizens and experts by surprise, resulting in extremely severe damage and loss of life. Existing methods based on local and regional information rarely go beyond national borders and cannot predict these floods well because of limited data on mega-floods, and because flood generation processes of extremes differ from those of smaller, more frequently observed events. Here we analyse river discharge observations from over 8000 gauging stations across Europe and show that recent mega-floods could have been anticipated from those previously observed in other places of Europe. Almost all observed mega-floods (95.5%) fall within the envelope values estimated from previous floods at other similar places on the continent, implying that local surprises are not surprising at the continental scale. This holds also for older events, indicating that mega-floods have not changed much in time relative to their spatial variability. The underlying concept of the study is that catchments with similar flood generation processes produce similar outliers. It is thus essential to transcend national boundaries and learn from other places across the continent to avoid surprises and save lives.

Main Text

Mega-floods that are much larger than floods experienced previously in a given catchment or region, can take citizens and local flood managers by surprise, resulting in catastrophic damage and loss of life. For example, the discharge of the July 2021 flood at the Rhine tributaries in Germany, and rivers in the Netherlands, Belgium and Luxembourg, was up to four times larger than any event on record in the region¹, causing almost 200 fatalities and damage in excess of \$40 billion. In this and other cases, the lack of previous local experience of events of this magnitude resulted in insufficient flood defence measures, preparedness and real-time response^{1,2}.

Because of their rare occurrence, mega-floods are difficult to predict. The standard method of estimating the magnitude of potential large floods consists of fitting a probability distribution to long series of flood observations, and extrapolating the distribution to small probabilities³. However, long series that include several exceptional events are rarely available. Some estimation methods use flood observations from neighbouring catchments⁴, to make up for the brevity of streamflow records which, however, rarely increases the chances of capturing mega-floods. Even when such events are observed, accurate discharge estimates are difficult to obtain as the flood wave may partially bypass the gauge and difficulties with extrapolating the rating curve. Moreover, the processes that generate extreme floods tend to differ from those that generate smaller and more frequent events⁵, making extrapolation notoriously inaccurate. One way of capturing changing flood processes with magnitude is through rainfall-runoff models, but they require long series of precipitation and are also subject to uncertainty^{6,7,8}. Large floods in historic or prehistoric times

(paleofloods) can also be used, although the information available is often not commensurate with the requirements of flood management^{9,10,11}.

An alternative for enhancing the accuracy of megaflood estimates is the transfer of flood information from hydrologically similar catchments where large events may have occurred⁴. In Europe the occurrence of megafloods is well documented at the national scale. The August 2002 flood in Germany, Austria and Bohemia was the largest in the last half century based on economic losses; the November 1994 Piedmont flood was the second costliest event in Europe between 1970 and 2020¹². Both events were caused by rainfall greater than one-third of the annual total, delivered in only 72 hours^{13,14}. However, flood information transfer rarely goes beyond national borders, and no previous study has examined megafloods in a systematic way across an entire continent, with the objective of learning from other places about the potential of future flood surprises. Some examples comparing the world's maximum measured floods also exist¹⁵, but they do not compare hydrologically similar catchments, which makes flood estimation less useful for practical purposes.

Anticipating megafloods

Here we analyse the most comprehensive dataset of annual maximum discharges in Europe available to date and show that recent megafloods could have been anticipated from observations in other parts of Europe, which would not be possible using national data only. We also show that the predictability of megafloods does not change in time when sub-periods are analysed. We base our analysis on annual maximum river discharge observations from 8023 gauging stations for the period 1810–2021. The average length of the series is 51.4 years and the catchment areas range between 1 km² and 800,000 km². Catchments across Europe are grouped into five hydroclimatic regions (Fig. 1) as a first step of identifying hydrologically similar catchments¹⁶. For each region, we estimate a regional envelope curve of flood discharges that represents the relationship between flood discharge and catchment area that is not exceeded by any observed flood in the region (see Methods; Extended Data Table 2). To examine possible changes in time, we also compare envelope curves obtained using observations from two 30-year sub-periods, i.e., 1961–1990 and 1991–2020.

We focus on 498 catchments (“target” catchments) where 510 recent (i.e. after 1999) megafloods that are surprising based on local data are identified (see Methods). To evaluate the possibility of anticipating megafloods in target catchments using information from other places in Europe, we perform a hindcast experiment of predicting their peak discharge with regional envelope curves, using flood observations from similar catchments up to the year before their occurrence. For each target catchment, a group of similar catchments (“donor” catchments) is identified in the corresponding hydroclimatic region based on the similarity of catchment area and the mean and coefficient of variation of the truncated flood series (up to the year before the megaflood). From this group of donor catchments we construct an envelope curve

which we compare with the megaflood that occurred later in the target catchments. We repeat this analysis for all 510 detected megafloods in the target catchments.

European envelope curves of flood discharges

Our data show that recent megafloods have occurred in all regions of Europe, although they are more frequent in the Atlantic and Continental regions (Fig.1; Extended Data Table 3), where respectively 8.7% and 7.2% of the catchments exhibit recent megafloods. In the Boreal region, the respective value is only 1.3%. The smaller value is related to the smaller interannual variability of floods in the Boreal region¹⁷.

In the Atlantic region, the megafloods (coloured points in Fig. 1b-f) are on average 3.4 times larger than the local mean annual maximum discharges (squares), while in the Continental and Mediterranean regions they are 5.3 and 5.2 times larger (Extended Data Table 3). The larger ratio in the Mediterranean is likely related to the more non-linear rainfall-runoff process and more variable precipitation in arid than in humid climates^{5,18}. However this analysis is not able to conclude whether megafloods are becoming more frequent or not.

The envelope curves defined by the largest floods also differ between hydroclimatic regions in terms of their intercept and slope (thick continuous lines in Fig. 1b-f; Extended Data Table 2). For a catchment size of 1000 km², the envelope specific discharge in the Mediterranean region is 5.26 m³s⁻¹km⁻² while in the Boreal region it is 1.37 m³s⁻¹km⁻². This is because the flood-inducing rainstorms in the Mediterranean are associated with much larger intensities than the flood-inducing snowmelt typical of Northern Europe. The slopes of the envelope curves are steepest in the Mediterranean area (-0.57) and flattest (-0.07) in the Boreal region (Fig. 1). This is because the Mediterranean rainstorms tend to be more localised than the snowmelt in the North of Europe. The envelope curves for the most recent sub-period (thin dotted lines) tend to be slightly lower than those for the first sub-period (thin dashed lines), except for the Mediterranean and the Atlantic region. The median regression curves (thin continuous lines) are slightly flatter than the respective envelopes, as larger catchments tend to have more regular flood regimes than small ones. Figs. 1g-j illustrate examples of flood series in pairs of catchments with and without megafloods.

To illustrate the potential of anticipating megafloods from other places in Europe, Fig. 2 shows three examples. The 2002 flood in the Kamp catchment in Austria (Fig. 2a) peaked at 459 m³s⁻¹ which is equivalent to a specific discharge of 0.74 m³s⁻¹km⁻² (black triangle) given the catchment area of 622 km². The envelope curve (blue line), defined by the hydrologically similar catchments within the hydroclimatic region, gives a specific discharge of 1.68 m³s⁻¹km⁻². This means that, in light of European floods, the Kamp was not at all surprising while for the locals it was¹⁹. The regional envelope discharge illustrated in Fig. 2 is defined based on previously observed floods in various European countries, including Bulgaria and Poland (blue circles in Fig. 2d).

The 2009 flood in the Cumbrian Derwent catchment in the UK (Fig. 2b) peaked at $0.84 \text{ m}^3\text{s}^{-1}\text{km}^{-2}$ and was 58% larger than the second largest event on record which occurred in 2005. The corresponding envelope specific discharge is $1.64 \text{ m}^3\text{s}^{-1}\text{km}^{-2}$. Much larger extremes were observed in similar catchments in Norway (Fig. 2e). The 2009 megaflood in the Derwent was itself exceeded in 2015, however this later event still lies below the envelope curve and was not as surprising as the 2009 event (11% larger)².

The 2021 flood in the Ahr catchment in Germany (Fig. 2c) peaked at $0.80 \text{ m}^3\text{s}^{-1}\text{km}^{-2}$, similar to the Kamp flood, with an envelope estimate of $1.57 \text{ m}^3\text{s}^{-1}\text{km}^{-2}$. For the Ahr catchment, the similar catchments making up the donor group are, in descending order of flood magnitude: the Timis in Romania, the Freiburger Mulde in Germany, the Maritsa in Bulgaria, the Ljig in Serbia, the Lausitzer Neisse in Germany, the Corrèze and Le Lot in France, the Nysa Kłodzka in Poland and the Birs in Switzerland (Fig. 3). Although each of these catchments has a specific hydrological behaviour, overall they can be considered hydrologically similar to the Ahr in terms of average climate and flood statistical properties. All of these ten catchments experienced record-breaking floods that were surprising based on previously observed events at that location, and these occurred in the period before 2021 (Fig. 3).

The analysis of Fig. 2 is repeated for all 510 recent megafloods in the target catchments in Europe (Fig. 4). In 95.5% of the target catchments, the discharge of the envelope is larger than that of the observed megaflood, suggesting that, from a European perspective, almost none of the events can be considered a regional surprise. In 9.6% of the cases, the observed megafloods are within 75% and 150% of the envelope (red points in Fig. 4a), i.e. the order of magnitude is similar. The target catchments are distributed all over Europe with a higher concentration in the West (Fig. 4b), reflecting positive trends in flood magnitudes in Western Europe^{20,21} and, to some degree, the higher station density.

The prediction is also conducted for 151 and 188 catchments with 151 and 190 recent (i.e. in the last 10 years of each sub-period) megafloods in the first and second sub-period, respectively. The distribution of the ratio between observed and predicted discharge (inset of Fig. 4a) indicates that there are no substantial changes in the predictability of megafloods in time. The discharge of the envelope is larger than that of the observed megaflood in 92% and 93.7% of the respective target catchments.

To evaluate the suitability of the donor selection, we compare the timing within the year of the target megafloods with that of the ten largest floods in the donor catchments (Fig. 4c). Flood timing is a proxy of flood generation processes²². Fig. 4c shows that the timing of the target megafloods (black lines) generally agrees with that of the donors (brown lines), both in terms of the average timing (angle from the centre of the circle) and the consistency of timing between events (distance to the centre). The agreement points towards the plausibility of the donor selection and prediction. A tendency for the observed timings to be more bimodal than the predictions is likely related to the smaller number of events.

246

247 **Implications of expanding the perspective**

248 Whereas previous studies have assessed the potential for megafloods mainly based
249 on local or regional data, this study expands the observation area to the continental
250 scale. We use megafloods that have occurred in hydrologically similar catchments
251 elsewhere on the continent as a surrogate for the megafloods that could happen in the
252 catchment of interest in the future.

253 The degree to which this transfer of information is possible depends on the suitable
254 choice of donor catchments based on the notion of hydrological similarity²³. The
255 underlying concept is that catchments with similar flood generation processes,
256 including rainfall, infiltration and flow paths, produce similar outliers, as these
257 processes determine the transition from smaller to larger events^{5,24,25}. Here we use
258 catchment area and the mean and coefficient of variation of the truncated flood series
259 within the same hydroclimatic region as a proxy of similarity in flood generation
260 processes. While other similarity measures exist¹⁶, our donor catchment selection is
261 deemed plausible because of the similarity of the timing within the year of the events,
262 given that timing is a fingerprint of the interplay between climatic and catchment
263 processes²². Additional spot testing of catchment pairs (such as the Ahr catchment in
264 Germany paired with the Timis catchment in Romania) based on prior knowledge from
265 the literature^{1,25} confirms the similarity. To assess robustness of the method we
266 conduct a sensitivity analysis on the parameters of the similarity criteria and the choice
267 of hydroclimatic regions (Extended Data Fig. 1-8). The results show that changing
268 parameters and/or regions may modify individual donor catchments, but the envelope
269 curve that arises from the set of donor catchments is affected much less (see method
270 section for details).

271 The cross-validation experiment conducted here, starting from observed megafloods,
272 withholding them and only using data from floods that have occurred previously,
273 mimics the case of anticipating megafloods that have not yet occurred. We show that
274 it is indeed feasible to estimate the order of magnitude of possible future megafloods.
275 Almost all observed megafloods (95.5%) are smaller than the envelope values
276 estimated, i.e. the local surprises are not surprising at the continental scale. Similar
277 results are found for different sub-periods, indicating that megafloods have not
278 changed much in time relative to their spatial variability within Europe. These findings
279 are in line with recent studies in the US showing little evidence for temporal trends of
280 large floods²⁶.

281 The proposed envelope curve approach complements alternative methods such as
282 regional statistical approaches that spatially interpolate observed discharges⁴ or
283 process-based rainfall-runoff modelling²⁷. These methods provide best estimates of
284 expected floods, while the envelope method reflects a possible worst case – which
285 itself is an important aspect of flood risk planning.

The focus on a possible worst case implies that the envelope values are generally too large to serve as design values for most types of flood defence infrastructure from a cost-benefit perspective. Rather, they describe a possibility space²⁸ that is prudent to consider as civil protection scenarios, required to organise local preparedness, and for testing the safety of very large dams. They can be used to derive extreme flood hazard scenarios, either failure scenarios (what can go wrong?) or future development scenarios (what could the future look like?) that could strengthen existing methods such as the Probable Maximum Flood (PMF) concept²⁹. There is an increasing need for considering the extremes of the extremes, as there is a tendency in society for smaller acceptable risks²⁹, so flood risk management should account for the potential of surprises and their devastating consequences. This requires a shift in thinking²⁹ and the application of envelope curves, storylines^{2,30} and compound event analyses³¹. Making individuals and societies more robust against surprises therefore goes beyond the design of spillways and flood management plans.

In summary, to anticipate megafloods we must learn from other places in order to reduce the surprise factor of their occurrence, increase flood risk awareness and enhance preparedness of flood risk management. To this end, it is essential to move beyond national flood risk assessment and share information on megafloods across countries and continents.

Acknowledgements

We acknowledge all flood data providers listed in Extended Data Table 1. G. Blöschl and M. Bertola were supported by the FWF projects ‘SPATE’ (I 3174, I 4776) and W1219-N22. B. Merz and B. Guse were supported by the DFG ‘SPATE’ project (FOR 2416). A. Viglione, P. Claps, D. Ganora, M. Borga and E. Dallan were supported by the European Union Next-GenerationEU ‘RETURN’ Extended Partnership (National Recovery and Resilience Plan – NRRP, Mission 4, Component 2, Investment 1.3 – D.D. 1243 2/8/2022, PE0000005). S. Kohnová and J. Szolgay were supported by the Slovak Research and Development Agency (number APVV-20-0374) and the VEGA Grant Agency (number 1/0782/21). J. Hannaford and S. Turner were supported by the ROBIN (Reference Observatory of Basins for INternational hydrological climate change detection) initiative, with funding from the Natural Environment Research Council (grant number NE/W004038/1). The authors acknowledge the involvement in the data screening process of M. Haas.

Author Contributions Statement

G. Blöschl and M. Bertola initiated the study and wrote the first draft of the paper. M. Bertola, G. Blöschl, M. Borga, A.C., P.C., E.D., D.G., A.M., A.V. and E.V. designed the study. M. Bertola collated the updated version of the database with the help of most of the co-authors and conducted the analyses. G. Blöschl, M. Bertola, interpreted the results in the context of underlying geophysical mechanisms. G. Boglarka, M. Boháč, A.C., S.K., O.L., S.L. M.M.-G., K.G., Z.G., B.G., J.K., B.M., P.M., J.P., L.P., I.R., K.S., J.S., P.V., P. Ward, P. Willems., and N.Ž. interpreted the results in central Europe. G.T.A., O.B., M. Borga, A.C., I.Č., G.B.C., P.C., E.D., D.G., A.G., A.M., L.M., D.O., M.Š., A.V. and E.V. interpreted the results in southern Europe. B.A., B.K., D.L., and N.V. interpreted the results in northern Europe. J.H., S.H., C.M., S.T., and E.S. interpreted the results in western Europe. I.D., N.F., L.G., M.K., J.K., M.O. and V.O. interpreted the results in eastern Europe. All authors contributed to framing and revising the paper.

Competing Interests Statement

The authors declare no competing interests.

Figure Captions

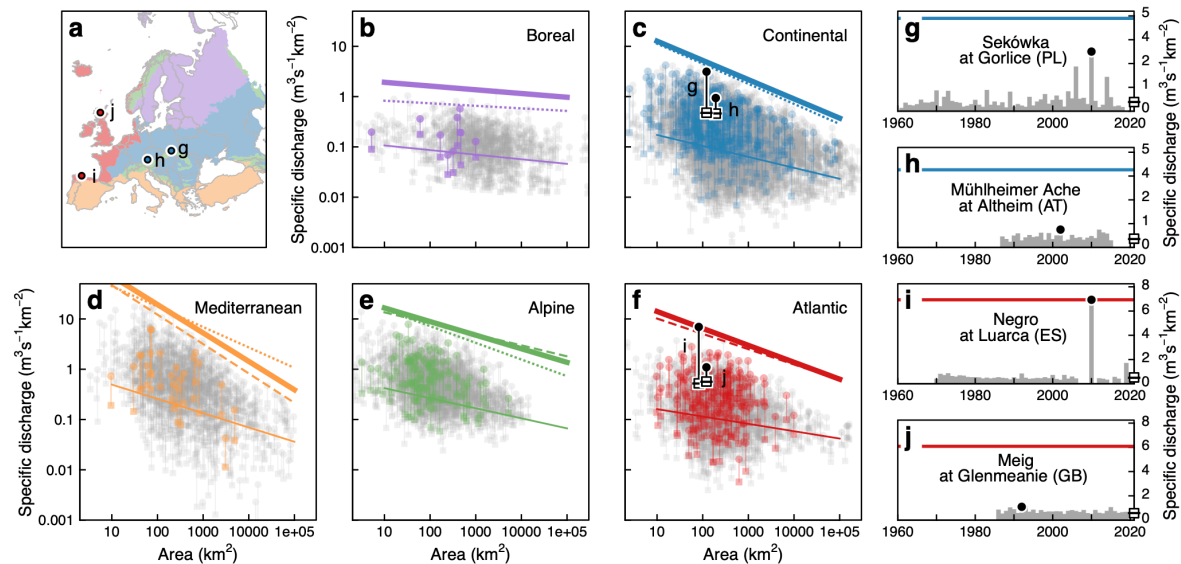


Fig. 1: Megafoods in Europe. (a) Five hydroclimatic regions: Boreal (purple), Continental (blue), Mediterranean (orange), Alpine (green) and Atlantic (red). (b-f) Maximum observed specific flood discharges (points) and mean of annual specific flood discharges (squares) over the entire observation period at each stream gauge as a function of catchment area. Regional envelope curves (thick lines) and median regional annual specific flood discharges (thin lines) for the full record period are shown for each hydroclimatic region. Envelope curves for two 30-year sub-periods are also shown (dashed lines for 1961-1990, dotted lines for 1991-2020). Parameters of the envelope curves are listed in Extended Data Table 2. Coloured symbols indicate the mean and maximum flood discharges in the 498 catchments with recent megafoods, grey points those of the remaining catchments. (g-j) Examples of series of annual flood discharges with (g and i) and without (h and j) megafoods; their corresponding mean (squares) and maximum values (points) are highlighted in black in (c) and (f). The locations of corresponding stream gauges are indicated in (a) by circles.

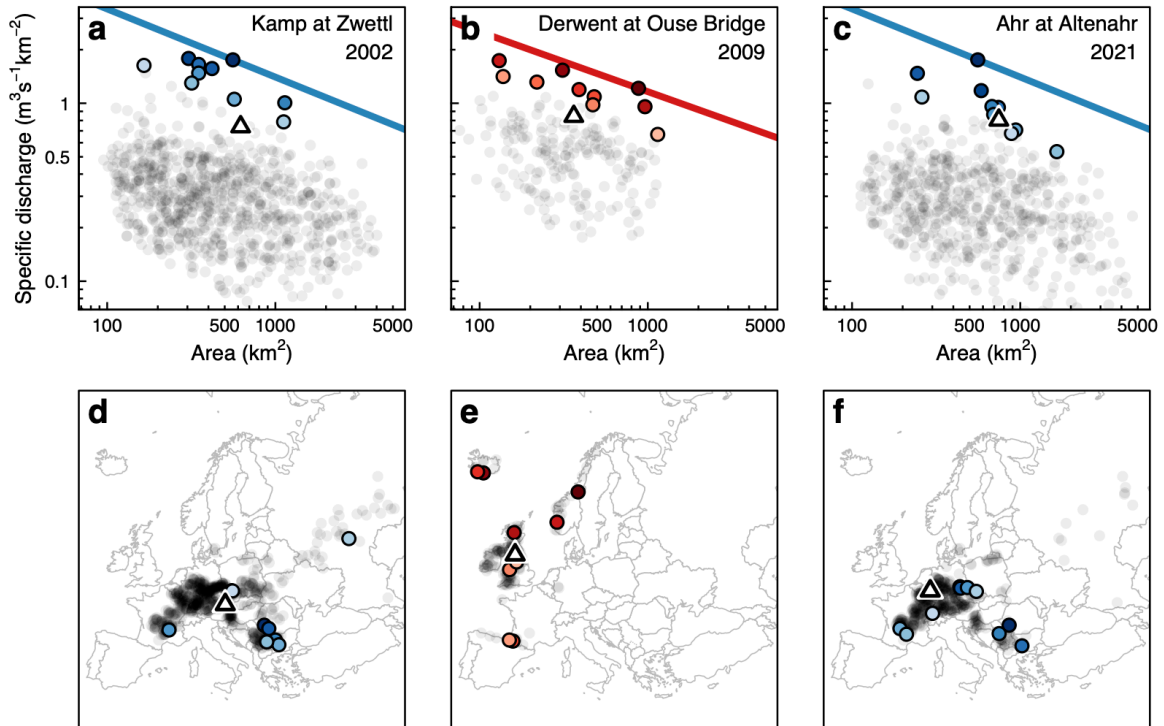


Fig. 2: Envelope curves for three catchments with recent mega-floods in Europe. (a,d) Kamp (622 km² catchment area) with 2002 flood; (b,e) Cumbrian Derwent (363 km²) with 2009 flood, and (c,f) Ahr (746 km²) with 2021 flood, indicated with triangles. (a-c) Maximum specific discharges observed before the year of occurrence of the mega-flood for 824 (a), 196 (b) and 590 (c) similar donor catchments (points) selected within the corresponding hydroclimatic region. Coloured points indicate ten largest events (in terms of distance to the envelope curve), with shades being darker for events that are closer to the envelope. Line shows resulting envelope curve with the slope estimated from the hydroclimatic regions (Fig. 1b-f). (d-f) Location of the target (triangle) and donor (points) catchments. Note that the envelope curves of Fig. 1 refer to the entire hydroclimatic region, while here they refer to the donor group within a region.

target catchments (black lines), and mean timing of the 10 largest floods in the donor catchments (coloured points) and their distribution (brown lines). The distance of the points to the centre is inversely proportional to the standard deviation of the flood timing.

References

1. Apel, H., Vorogushyn, S., & Merz, B. Brief communication–Impact Forecasting Could Substantially Improve the Emergency Management of Deadly Floods: Case Study July 2021 floods in Germany. *Natural Hazards and Earth System Sciences Discussions*, 1-10 (2022).
2. Kreibich, H., Van Loon, A.F., Schröter, K. et al. The challenge of unprecedented floods and droughts in risk management. *Nature* 608, 80–86 (2022).
3. De Niel, J., Demarée, G., Willems, P. Weather typing based flood frequency analysis validated for exceptional historical events of past 500 years along the Meuse river, *Water Resources Research*, 53(10), 8459-8474 (2017).
4. Robson, A. J. and Reed, D. W. Flood Estimation Handbook (FEH), chap. Statistical procedures for flood frequency estimation, p. Vol. 3, Institute of Hydrology, Wallingford, UK (1999).
5. Rogger, M., Pirkl, H., Viglione, A., Komma, J., Kohl, B., Kirnbauer, R., Merz, R., & Blöschl, G. (2012). Step changes in the flood frequency curve: Process controls. *Water Resources Research*, 48(5), 1–15.
6. Bergstrand M., Asp S. and Lindström G. Nationwide hydrological statistics for Sweden with high resolution using the hydrological model S-HYPE. *Hydrology Research*, 45.3, 349-356 (2014).
7. Devitt, L., Neal, J., Wagener, T., & Coxon, G. Uncertainty in the extreme flood magnitude estimates of large-scale flood hazard models. *Environmental Research Letters*, 16(6), 064013 (2021).
8. Bouaziz, L. et al. Behind the scenes of streamflow model performance, *Hydrol. Earth Syst. Sci.*, 25, 1069–1095 (2021).
9. Kjeldsen, T.R. et al. Documentary evidence of past floods in Europe and their utility in flood frequency estimation. *Journal of Hydrology*, 517, 963–973 (2014).
10. Blöschl, G., Kiss, A., Viglione et al. Current European flood-rich period exceptional compared with past 500 years. *Nature*, 583(7817), 560–566 (2020).
11. U.S. Geological Survey Scientific Investigations Report 2020–5065, 89 p. (2020).
12. World Meteorological Organisation (WMO). WMO Atlas of Mortality and Economic Losses from Weather, Climate and Water Extremes (1970–2019). WMO-No. 1267 (2021).
13. Blöschl, G., Nester, T., Komma, J., Parajka, J., & Perdigão, R. A. P. The June 2013 flood in the Upper Danube Basin, and comparisons with the 2002, 1954 and 1899 floods. *Hydrology and Earth System Sciences*, 17(12), 5197–5212 (2013).
14. Lionetti, M. The Italian floods of 4–6 November 1994. *Weather*, 51(1), 18-27 (1996).
15. Herschy, R. W. (2002). The world's maximum observed floods. *Flow Measurement and Instrumentation*, 13(5–6), 231–235. [https://doi.org/10.1016/S0955-5986\(02\)00054-7](https://doi.org/10.1016/S0955-5986(02)00054-7)
16. Kuentz, A., Arheimer, B., Hundecha, Y., and Wagener, T. Understanding hydrologic variability across Europe through catchment classification, *Hydrol. Earth Syst. Sci.*, 21, 2863-2879 (2017)

17. Lun, D., Viglione, A., Bertola, M., Komma, J., Parajka, J., Valent, P., & Blöschl, G. Characteristics and process controls of statistical flood moments in Europe – a data-based analysis. *Hydrology and Earth System Sciences*, 25(10), 5535–5560 (2021).
18. Blöschl, G. Flood generation: process patterns from the raindrop to the ocean, *Hydrol. Earth Syst. Sci.*, 26, 2469–2480 (2022)
19. Blöschl, G. Flood warning - on the value of local information. *International Journal of River Basin Management*, 6 (1), pp. 41-50 (2008).
20. Blöschl, G., Hall, J., Viglione, A. et al. Changing climate both increases and decreases European river floods. *Nature*, 573(7772), 108–111 (2019).
21. Bertola, M., Viglione, A., Lun, D., Hall, J., & Blöschl, G. Flood trends in Europe: are changes in small and big floods different? *Hydrology and Earth System Sciences*, 24(4), 1805–1822 (2020).
22. Blöschl, G., Hall, J., Parajka, J., Perdigão, R. A., Merz, B., Arheimer, B., ... & Živkoviæ, N. Changing climate shifts timing of European floods. *Science*, 357(6351), 588-590 (2017).
23. Blöschl, G., Sivapalan, M., Wagener, T., Viglione, A., Savenije, H.H. *Runoff Prediction in Ungauged Basins – Synthesis across Processes, Places and Scales*. Cambridge University Press (2013).
24. Kemter, M., Merz, B., Marwan, N., Vorogushyn, S., & Blöschl, G. Joint Trends in Flood Magnitudes and Spatial Extents Across Europe. *Geophysical Research Letters*, 47(7), 1–8 (2020).
25. Popescu, I., Jonoski, A., Van Andel, S. J., Onyari, E., & Moya Quiroga, V. G. Integrated modelling for flood risk mitigation in Romania: case study of the Timis–Bega river basin. *International journal of river basin management*, 8(3-4), 269-280 (2010).
26. Collins, M. J., Hodgkins, G. A., Archfield, S. A., & Hirsch, R. M. (2022). The occurrence of large floods in the United States in the modern hydroclimate regime: Seasonality, trends, and large-scale climate associations. *Water Resources Research*, 58, e2021WR030480. <https://doi.org/10.1029/2021WR030480>
27. Donnelly, C, Andersson, J.C.M. and Arheimer, B. Using flow signatures and catchment similarities to evaluate a multi-basin model (E-HYPE) across Europe. *Hydr. Sciences Journal* 61(2):255-273 (2016)
28. Sivapalan, M., & Blöschl, G. Time scale interactions and the coevolution of humans and water. *Water Resources Research*, 51(9), 6988–7022 (2015).
29. Merz, B., Vorogushyn, S., Lall, U., Viglione, A., & Blöschl, G. Charting unknown waters-On the role of surprise in flood risk assessment and management. *Water Resources Research*, 51(8), 6399–6416 (2015).
30. Shepherd, T. G. Storyline approach to the construction of regional climate change information. *Proceedings of the Royal Society A*, 475(2225), 20190013 (2019).
31. Thieken, A. H., Samproгна Mohor, G., Kreibich, H., and Müller, M.: Compound inland flood events: different pathways, different impacts and different coping options, *Nat. Hazards Earth Syst. Sci.*, 22, 165–185 (2022).

Methods

Datasets

The hydrological data used in this study were obtained from a pan-European Flood Database³² with subsequent updates. The current version contains data from 8,023 hydrometric gauging stations from 68 European data sources for the period 1810–2021 (Extended Data Table 1). The dataset consists of the highest discharge (daily mean or instantaneous discharge) in each calendar year for each station. The stations are located within the domain bounded by 22.25° W–63.25° E and 34.25° N–71.25° N (Extended Data Fig. 1), and catchment areas range between 1 km² and 800,000 km². The dataset was screened for data errors. The screening involved visual examination of the flood records, analysis of flood seasonality and examination of the gauge location and catchment area in Google Maps. All available stations, including those affected by reservoir construction, were considered for the analysis because reservoir effects were deemed to have little significance for envelope curves for large hydroclimatic regions. Similarly, all available years with data were considered notwithstanding differences in the record lengths, because the focus was on the maxima observations of each series. The minimum series length is 10 years, and the average length is 51.4 years.

The gauging stations were grouped into five regions (Fig. 1a; Extended Data Fig.1) that reflect similar hydroclimatic conditions by generalising the European Biogeographical regions³³ with a view on flood processes. The Steppic and Pannonian regions were merged with the Continental region, the Arctic region with the Boreal region, and the Anatolian and Black Sea regions with the Mediterranean region. Additionally, part of northern Italy was considered as part of the Mediterranean region and Iceland as part of the Atlantic region. For comparison, an alternative subdivision of Europe into five regions¹⁷ was considered in a sensitivity analysis (Extended Data Fig. 4a). In order to examine possible changes, the observation period was subdivided into two 30-year sub-periods, P1 (1961–1990) and P2 (1991–2020).

Regional envelope curves

We quantified the largest flood events in each region by scaling the peak discharges by catchment area via envelope curves that represent the upper limit of the dataset (Fig. 1):

$$\log(q) = a + b \cdot \log(A) \quad (1)$$

where q (m³s⁻¹km⁻²) is the specific discharge, i.e. the discharge per unit catchment area A . The parameter b was estimated by quantile regression with quantile $z=0.999$ using the `rq` function of the R `quantreg` package^{34,35}. The quantile regression enables a more robust estimate than the tangents on the maxima, because it uses the complete dataset rather than the maxima only. The intercept a was determined such that it

satisfies the envelope condition, i.e. the envelope curve is the upper bound of all observed flood discharges in a region (Extended Data Table 2). For comparison, a quantile regression with $z=0.5$ is also shown in Fig. 1 (thin line).

Megafoods

For the selection of recent megafoods (Fig. 4) the following criteria were adopted:

(i) the discharge value is a high outlier in the corresponding series of annual maximum flood discharges, according to the definition³⁶:

$$q_{mf} > Q_3 + k * (Q_3 - Q_1) \quad (2)$$

where Q_1 and Q_3 are the first and third quartile (i.e. respectively 25% and 75% of the observations lies below this values) and $k=3$;

(ii) the discharge value is record-breaking and locally surprising, i.e., its return period T_{mf} is at least 3 times larger than the return period of the second largest event up to that year T_{sl} . The return period was obtained by fitting a GEV distribution to each flood series up to the year of the megafood using the L-moments (R extRemes package).

(iii) it occurred after the year 1999 (when the full observation period is analysed) and the corresponding series has at least 20 years of data previous to the event.

The selection resulted in a set of 510 megafoods from 498 target catchments, whose observed specific discharge and location of corresponding gauges are shown in Fig. 4a and 4b. When detecting megafoods in the two 30-year sub-periods, only observations within each sub-period are considered and the criterion (iii) is modified such that events in the last 10 years of the respective sub-period are selected (i.e. after 1979 for P1 and after 2009 for P2).

We tested the robustness of the results to the criterion (i) for the selection of high outliers, using the definition for skewed data³⁷:

$$\begin{cases} q_{mf} > Q_3 + 1.5e^{3MC} IQR & \text{if } MC > 0 \\ q_{mf} > Q_3 + 1.5e^{4MC} IQR & \text{if } MC < 0 \end{cases} \quad (3)$$

Where MC is the medcouple³⁸, a robust measure of skewness, defined as:

$$MC(X_n) = \text{med}_{x_i \leq m_n \leq x_j} h(x_i, x_j) \quad (4)$$

with m_n is the sample median of X_n and

$$h(x_i, x_j) = \frac{(x_j - m_n) - (m_n - x_i)}{x_j - x_i} \quad (5)$$

The alternative selection resulted in a set of 677 megafoods (Supplementary Fig. S1), whose observed specific discharge and location of corresponding gauges are shown in Supplementary Fig. S2.

We also tested the sensitivity of the results to criterion (ii) for the selection of record-breaking and surprising events, by varying the threshold T_{mf}/T_{sl} between 1 and 4. The results of the sensitivity analysis are shown in Supplementary Fig. S3 and indicate that, when the definition of megafloods is extended to less surprising events (i.e. $T_{mf}/T_{sl} < 3$), the fraction of megafloods larger than the envelope is unchanged. The only exception is the Boreal region, where fewer events are selected.

Donor catchments

For each catchment in which a megaflood had occurred (target catchment), a pool of similar catchments (donor catchments) was identified in the same region. The similarity between the catchments was quantified in terms of weighted normalised Euclidean distance D in a three-dimensional space with the following dimensions: the logarithm of catchment area A , the logarithm of the mean of the annual maximum specific discharges q_m normalised to a catchment area of 100km², and the coefficient of variation CV of the annual maximum discharges:

$$D = \sqrt{\alpha \left(\frac{\log A_i - \log A_j}{sd(\log A)} \right)^2 + \beta \left(\frac{\log q_{m,i} - \log q_{m,j}}{sd(\log q_m)} \right)^2 + \gamma \left(\frac{CV_i - CV_j}{sd(CV)} \right)^2} \quad (6)$$

where i refers to the target catchment, j to a potential donor catchment and sd is the standard deviation of all catchments in the donor group. Greek letters indicate weights. q_m and CV were calculated on flood data prior to the year of occurrence of the target event to obtain a cross-validation experiment that resembles a case of anticipating megafloods a priori. In estimating q_m and CV we excluded outliers (for both the target and the donor catchments) according to the criterion of Eq. (2), because megafloods should not influence the comparison, and only smaller, frequently occurring floods were used, which is the only information usually available in the case of a prediction. In selecting the number of catchments in the pooling group, there is a tradeoff between a larger group that has a higher chance of containing very large floods, and a smaller group that is hydrologically more homogeneous. For Fig. 1, 2, 3 we used $\alpha=\beta=\gamma=1$ (corresponding to the assumption of the three dimensions having the same importance) and included catchments with $D < D_{max}$ with $D_{max}=1$, guided by a sensitivity analysis (see below and Extended Data Fig. 2).

Megaflood prediction

We repeated the selection of the donor group for each target catchment and estimated the envelope curve, using the slope b of the corresponding hydroclimatic region and the intercept determined as the minimum that satisfies the envelope condition of the group only. The procedure only uses observations from donor catchments up to the year before the megaflood in the target catchment (Fig. 2a-c). We finally obtained an estimate of the discharge of a potential megaflood in the target catchment (predicted

mega-flood) from the envelope curve and compared it to the discharge of the observed mega-flood (Fig. 4a).

In order to evaluate the plausibility of the donor selection we analysed the timing of the mega-floods observed in the target and donor catchments using previously established methods²² (Fig. 4c). We compared the distribution of the timing of the observed mega-floods to the average timing of the 10 largest floods in the donor group. The circular distributions in Fig. 4c were obtained using the R circular package.

In order to evaluate the robustness of the method we conducted a number of sensitivity analyses. We varied D_{max} between 0.5 and 1.5 and showed that an increase in D_{max} translates into an increasing number of target mega-floods that are below the envelope (Extended Data Fig. 2). The larger fraction in the Boreal region is because of fewer donors available compared to the other regions. We also tested the sensitivity of α , β and γ , examining four weight combinations: equal weights ($\alpha=\beta=\gamma=1$) and doubling one of the weights ($\alpha=2$ and $\beta=\gamma=1$; $\alpha=\gamma=1$ and $\beta=2$; $\alpha=\beta=1$ and $\gamma=2$), which corresponds to the hypothesis of one dimension being more important than the others in the donor selection. There is very little effect on the number of target mega-floods below the envelope (Extended Data Fig. 3). While a different set of parameters may modify some of the donor catchments, the resulting envelope curve changes very little. Finally we tested the effect of replacing the regional subdivision of Fig. 1 by an alternative subdivision¹⁷. The analysis shows that the alternative regions may modify the choice of individual donor catchments but, again, the overall conclusions do not change (Extended Data Fig. 4-7).

Data availability

The flood discharge data from the data holders/sources listed in Extended Data Table 1 that were used in this paper are available at <https://github.com/tuwhydro/mega-floods>.

Code availability

The data analysis was performed in R using the supporting packages circular, lubridate, plotrix, quantreg, raster, RColorBrewer, rgdal, rworldmap and scales. The code used can be downloaded from <https://github.com/tuwhydro/mega-floods>.

Methods-only references

32. Hall, J. et al. A European Flood Database: facilitating comprehensive flood research beyond administrative boundaries. Proc. Int. Assoc. Hydrol. Sci. 370, 89–95 (2015)

- 614 33. Roekaerts, M.: The biogeographical regions map of Europe, in: Basic principles of its creation
615 and overview of its development, European Environment Agency, Copenhagen, available at:
616 [https://www.eea.europa.eu/data-and-maps/ data/biogeographical-regions-europe-3](https://www.eea.europa.eu/data-and-maps/data/biogeographical-regions-europe-3) (2002).
- 617 34. Koenker, R. W. Quantile Regression, Cambridge U. Press (2005).
- 618 35. Amponsah, W., Marra, F., Marchi, L., Roux, H., Braud, I., Borga, M. Objective Analysis of
619 Envelope Curves for Peak Floods of European and Mediterranean Flash Floods. In: Leal
620 Filho, W., Nagy, G., Borga, M., Chávez Muñoz, P., Magnuszewski, A. (eds) Climate Change,
621 Hazards and Adaptation Options. Climate Change Management. Springer, Cham (2020).
- 622 36. Tukey JW. Exploratory Data Analysis. Reading (Addison-Wesley): MA, 1977.
- 623 37. Hubert, M., & Vandervieren, E. (2008). An adjusted boxplot for skewed
624 distributions. Computational statistics & data analysis, 52(12), 5186-5201.
- 625 38. Brys G, Hubert M, Struyf A. A robust measure of skewness. J. Comput. Graph. Stat. 2004;
626 13: 996–1017.